Decreased miR-92a-3p expression potentially mediates the pro-angiogenic effects of oxidative stress-activated endothelial cell-derived exosomes by targeting tissue factor

SUFANG LI[1-3], LAN YUAN[4], LINA SU[1-3], ZHENG LIAN[1-3], CHUANFEN LIU[1-3], FENG ZHANG[1-3], YUXIA CUI[1-3], MANYAN WU[1-3] and HONG CHEN[1-3]

[1]Department of Cardiology, Peking University People's Hospital; [2]Beijing Key Laboratory of Early Prediction and Intervention of Acute Myocardial Infarction, Peking University People's Hospital; [3]Center for Cardiovascular Translational Research, Peking University People's Hospital, Beijing 100044; [4]Medical and Healthy Analytical Center, Peking University, Beijing 100191, P.R. China

Received May 14, 2020; Accepted August 5, 2020

DOI: 10.3892/ijmm.2020.4713

Abstract. Angiogenesis is an essential pathological feature of vulnerable atherosclerotic plaque. Exosome-derived microRNAs (miRNAs or miRs) have been proven to be important regulators of angiogenesis. However, the role of exosomes, which are secreted by endothelial cells (ECs) under conditions of oxidative stress, in angiogenesis remain unclear. The present study aimed to investigate the effects and mechanism of oxidative stress-activated endothelial-derived exosomes in angiogenesis. Exosomes were isolated from H_2O_2-stimulated human umbilical vein ECs (HUVECs; termed Exo$^{-H_2O_2}$) by differential centrifugation and characterized by transmission electron microscopy, nanoparticle tracking analysis and western blot analysis. Exo$^{-H_2O_2}$ enhanced HUVEC proliferation, migration and tube formation, as determined by EdU incorporation assay, scratch wound migration assay and tube formation assay, respectively. miR-92a-3p was identified as the predominantly downregulated miRNA in the Exo$^{-H_2O_2}$-treated HUVECs by small RNA sequencing, and the expression of primary miR-92a (pri-miR-92a-1) was also decreased, as shown by RT-qPCR. Similarly, the inhibition of miR-92a-3p promoted angiogenesis *in vitro* and *in vivo*. miR-92a-3p overexpression blocked the pro-angiogenic effects of Exo$^{-H_2O_2}$ on target ECs. Tissue factor (TF), a molecule involved in angiogenesis, was increased in HUVECs in which miR-92a-3p expression was downregulated, as shown by mRNA sequencing. TF was also predicted as a target of miR-92a-3p by using the RNAhybrid program. The overexpression or suppression of miR-92a-3p modified TF expression at both the mRNA and protein level, as measured by RT-qPCR and western blot analysis, respectively. Luciferase reporter assays suggested that miR-92a-3p inhibited TF expression by binding to the 3' untranslated region of TF. On the whole, the findings of the present study demonstrate that exosomes released from oxidative stress-activated ECs stimulate angiogenesis by inhibiting miR-92a-3p expression in recipient ECs, and TF may be involved in the regulatory effects of miR-92a-3p on angiogenesis.

Correspondence to: Dr Hong Chen, Department of Cardiology, Peking University People's Hospital, 11 Xizhimen South Street, Xicheng, Beijing 100044, P.R. China
E-mail: chenhongbj@medmail.com.cn

Key words: endothelial cells, exosomes, angiogenesis, miR-92a-3p, tissue factor

Introduction

A functionally and structurally intact vascular endothelium is essential for maintaining the normal function and activity of the cardiovascular system. Continuous stimulation (e.g., stress, inflammation and hypoxia) can cause vascular endothelial activation and injury, eventually leading to atherosclerosis (1,2). Angiogenesis, mainly manifested as endothelial cell (EC) proliferation, migration and tube formation, is an essential pathological process of atherosclerosis (3). Understanding the regulatory mechanisms of angiogenesis during endothelial activation and injury is crucial for controlling the progression of atherosclerosis.

Exosomes, with a size of 50 to 150 nm, are produced by most cell types and contain a wide range of functional proteins, lipids, messenger RNAs (mRNAs) and microRNAs (miRNAs or miRs) (4). Increasing evidence has indicated that the physiological functions of EC can be regulated by exosomes shed from various types of cells (5-9). In particular, ECs secrete functional exosomes, which can in turn affect the physiological behavior of recipient ECs by delivering miRNAs or proteins (10,11). In spite of extensive studies, the effects and mechanisms underlying the communication between vascular ECs during exosome-mediated angiogenesis remain to be fully elucidated. As one of the key pathogenetic factors of angiogenesis during atherosclerosis, oxidative stress can induce angiogenesis via vascular endothelial growth factor-dependent/independent signaling pathways (12). However, the role and mechanisms of exosomes secreted by oxidative stress-stimulated ECs in angiogenesis remain unclear.

miRNAs are a class of small non-coding RNAs that post-transcriptionally suppress gene expression by binding to the 3' untranslated region (3'UTR) of target mRNAs. Several miRNAs have been shown to regulate vascular endothelial function and angiogenesis (13), and miR-92a is most closely related to these processes (14-19). The overexpression of miR-92a in ECs has been shown to block angiogenesis by targeting several pro-angiogenic proteins (14). In the present study, through high-throughput screening, it was found that miR-92a-3p was markedly downregulated and was the most abundant miRNA differentially expressed in ECs treated with oxidative stress-stimulated EC-derived exosomes. It was also demonstrated that exosomes shed from oxidative stress-stimulated ECs enhanced EC proliferation, migration and angiogenesis by decreasing miR-92a-3p expression in target ECs. Moreover, it was confirmed that tissue factor (TF) was a novel target gene of miR-92a-3p, which may mediate the regulatory role of miR-92a-3p in angiogenesis.

Materials and methods

Cells and cell culture. Human umbilical vein ECs (HUVECs) and 293 cells were purchased from the Shanghai Institutes for Biological Sciences (CAS). HUVECs were cultured in endothelial cell medium (ECM) supplemented with 5% fetal bovine serum (FBS), 1% endothelial cell growth supplement (ECGS), penicillin (100 U/ml) and streptomycin (100 mg/ml) (Sciencell, Inc.). When HUVEC confluency reached approximately 70-80%, FBS in ECM was replaced by 5% exosome-free FBS (System Biosciences) and HUVECs were stimulated with or without 100 μM H_2O_2 for 24 h to produce exosomes. HUVECs incubated with exosomes were all cultured in basal medium (without FBS). 293 cells were cultured in Dulbecco's modified Eagle's medium (DMEM) containing 10% FBS, penicillin (100 U/ml) and streptomycin (100 μg/ml). All the cells were cultured in a 5% CO_2 incubator at 37˚C (Thermo Fisher Scientific, Inc.).

miRNA transfection. HUVECs at 70-80% confluency were transfected with miR-92a-3p inhibitor (66.7 nM), miR-92a-3p mimic (40.0 nM), a negative control (NC) inhibitor or NC mimic (Suzhou Genepharma Co., Ltd.), respectively, using Lipofectamine 2000 (2.7 μg/ml for inhibitor, 1.3 μg/ml for mimic) (Invitrogen; Thermo Fisher Scientific, Inc.). The sequences of miR-92a-3p/NC mimic or inhibitor were as follows: miR-92a-3p inhibitor, 5'-ACAGGCCGGGACAAG UGCAAUA-3'; miR-92a-3p mimic, 5'-UAUUGCACUUGU CCCGGCCUGU-3' and 5'-AGGCCGGGACAAGUGCAA UAUU-3'; NC inhibitor, 5'-CAGUACUUUUGUGUAGUA CAA-3'; NC mimic, 5'-UUCUCCGAACGUGUCACGUTT-3' and 5'-ACGUGACACGUUCGGAGAATT-3'. Following 24 or 48 h of transfection, the cells were harvested or further treated with exosomes according to the different experimental purposes.

Exosome isolation. Endothelial exosomes in the conditioned medium were isolated by differential centrifugation, as previously described (20). The medium was centrifuged at 300 x g for 10 min, 2,000 x g for 10 min and 10,000 x g for 30 min at 4˚C. The supernatant was then filtered through a 0.22-μm filter (EMD Millipore) to remove cellular debris, followed by ultracentrifugation at 100,000 x g and 4˚C for 70 min (WX+ Ultra series; Thermo Fisher Scientific, Inc.). The exosome pellets were washed with phosphate-buffered saline (PBS), followed by a second ultracentrifugation at 100,000 x g and 4˚C for 70 min, after which the exosomes were resuspended in PBS and stored at -80˚C.

Transmission electron microscopy. Exosome morphology was observed using a transmission electron microscope (TEM). A total of 20 μl of samples were dropped onto a carbon-coated grid, which was then baked at 60˚C for 5 min using a polymerizer (ZB-J0010; Beijing Zhongxing Bairui Technology Co., Ltd.). The excess liquid was absorbed using filter paper. The grid was subsequently stained with 2% tungstophosphoric acid for 5 min. Following 2 washes with distilled water, the grid was baked again at 60˚C and visualized using a TEM at 80 kV (JEM-1400; Jeol, Ltd.).

Nanoparticle tracking analysis. The particle size of the exosomes was analyzed by nanoparticle tracking analysis (NTA) using ZetaView PMX110 (Particle Metrix GmbH) in the size mode. Exosome samples were diluted to the working range (10^6-10^9 particles/ml) of the detecting system with PBS. The video of the Brownian motion of particles was captured at 11 positions and the particle size was measured using ZetaView 8.02.28 software.

Exosome labeling. Exosomes were labeled with the red fluorescent dye, PKH26, according to manufacturer's instructions with minor modifications (Sigma-Aldrich; Merck KGaA) (20). A total of 2 μg of exosomes were rapidly mixed with 1 ml of PKH26 solution (PKH26 dye: Diluent C, 1:50 dilution). Following 5 min of incubation at 37˚C, 5 ml of whole ECM medium containing 5% exosome-free FBS were added to terminate the labeling reaction. The labeled exosomes were washed with PBS and centrifuged at 100,000 x g and 4˚C for 1 h. Exosome pellets were resuspended in 200 μl of PBS. Subsequently, the labeled exosomes were added to HUVECs and incubated for 12 h in a 5% CO_2 incubator at 37˚C (Thermo Fisher Scientific, Inc.) . Following incubation, the HUVECs were washed twice and fixed with 4% paraformaldehyde at room temperature for 15 min. The cells were washed 3 times and treated with 0.2% Triton X-100 at 37˚C for 15 min. Following 2 more washes, the cells were stained with 10 μg/ml of 4,6 diamidino-2-phenylindole (DAPI) for 5 min and then imaged under a confocal laser scanning microscope (Leica TCS SP5, Leica Microsystems GmbH).

Small RNA sequencing analysis. Following 24 h of incubation with exosomes, HUVECs were collected and total RNA were extracted using the miRNeasy Mini kit (Qiagen, Inc.). NEBNext® Multiplex Small RNA Library Prep Set for Illumina® (New England Biolabs, Inc.) was used to generate the sequencing library according to the manufacturer's instructions. Briefly, NEB 3' SR adaptors were ligated to the 3' end of small RNA and SR RT Primer hybridized to the excessive 3' SR adaptor. The 5' adapters were then ligated to the 5' ends of small RNA. M-MuLV Reverse Transcriptase (RNase H^-) was used to synthesize the first-strand cDNA. LongAmp Taq 2X

Master Mix, SR Primer for illumina and index (X) primer were used for PCR amplification. The PCR products corresponding to 140-160 bp were enriched to generate the cDNA library. Library quality was assessed on an Agilent 2200 system with DNA High Sensitivity Chips. The clustering of index-coded samples was carried out on a cBot Cluster Generation System using the TruSeq SR Cluster kit v3-cBot-HS (Illumina, Inc.) following the manufacturer's instructions. The sequencing (for 50-base read length) of cDNA library was performed on an Illumina Hiseq 2500. The clean data were obtained by trimming adaptor sequences and removing low-quality reads. The small RNA tags were aligned using Bowtie and mapped to the human genome reference (version: GRCh38 NCBI). miRBase20.0 was used as reference to obtain known miRNAs. Software mirdeep2 and miREvo were integrated to identify novel miRNAs. Differentially expressed miRNAs were analyzed using the DESeq R package (1.8.3). miRNAs with a P-value <0.05 were considered to exhibit a significant differential expression. miRNAs with similar expression pattern were clustered and displayed as a heatmap.

Messenger RNA (mRNA) sequencing analysis. HUVECs were transfected with miR-92a-3p inhibitor for 48 h and then total RNA were isolated using the miRNeasy Mini kit (Qiagen, Inc.). The NEBNext® Ultra™ Directional RNA Library Prep kit for Illumina® (New England Biolabs, Inc.) was used to generate the sequencing library according to the manufacturer's instructions. Briefly, mRNA was fragmented into 150-200 bp using divalent cations at 94˚C for 8 min. The cleaved mRNA fragments were reverse-transcribed into first-strand cDNA, and the fragments were end repaired and ligated with indexed adapters. Target bands were harvested through AMPure XP Beads (Beckman Coulter, Inc.). The products were purified and enriched by PCR to generate the final cDNA libraries and quantified by Agilent 2200. The tagged cDNA libraries were pooled in equal ratio and used for 150 bp paired-end sequencing in a single lane of the Illumina HiSeqXTen. To obtain clean data, raw reads were processed by removing the adaptor sequences, reads with >5% ambiguous bases and low-quality reads containing >20% of bases with qualities of <20. The sequencing data were aligned to human genome (version: GRCh38 NCBI) using the hisat2 algorithm. HTseq was used to count gene and the reads per kilobase per million mapped reads (RPKM) method was used to determine gene expression. Differentially expressed genes were analyzed using the DESeq2 algorithm with a fold change of >1.5 or <0.5, a P-value <0.05 and a false discovery rate of <0.05.

Reverse transcription-quantitative PCR (RT-qPCR). Total RNA was isolated from the HUVECs or exosomes using the miRNeasy Mini kit (Qiagen, Inc.). miRNA-specific stem-loop primers and the TaqMan MicroRNA Reverse Transcription kit (Applied Biosystems, Inc.) were used for the amplification of mature miRNAs. The expression level of mature miR-92a-3p was normalized to the expression levels of RNU6B in HUVECs and synthetic *C. elegans* miR-39 (cel-miR-39) (10 fmol/sample) (Qiagen, Inc.) in exosomes, respectively. The ImProm-II™ Transcription System and GoTaq 2-Step RT-qPCR System (Promega Corporation) were used for TF amplification. The TF expression level was normalized to the expression of GAPDH. The sequences of the primers were as follows: TF forward, 5'-GCCAGGAGAAAGGGGAAT-3' and reverse, 5'-CAGTGC AATATAGCATTTGCAGTAGC-3'; GAPDH forward, 5'-GAG TCAACGGATTTGGTCGT-3' and reverse, 5'-GACAAGCTT CCCGTTCTCAG-3'. The amplifications were performed as previously described (21). For the quantification of primary miR-92a, the levels of pri-miR-92a-1 and pri-miR-92a-2 were measured using the High Capacity cDNA Reverse Transcription kit (Applied Biosystems, Inc.), TaqMan Pri-miRNA assays (pri-miR-92a-1 assay ID: Hs03302603_pri, pri-miR-92a-2 assay ID: Hs03295977_pri) and TaqMan Gene Expression Master Mix (Applied Biosystems, Inc.) according to the manufacturer's instructions. The amplification conditions were pre-incubation at 95˚C for 10 min, followed by 40 cycles of 95˚C for 15 sec and 60˚C for 1 min. The results were normalized to the expression of GAPDH (TaqMan assay ID: Hs02758991_g1). qPCR was performed on an Applied Biosystems system (ViiA7) and all data are expressed as $2^{-\Delta\Delta Cq}$ (22).

Western blot analysis. HUVECs or exosome samples were lysed using a RIPA buffer (Solarbio, Inc.) and then centrifuged at 12,000 x g and 4˚C for 15 min. The supernatant was collected and the protein concentration was measured using the bicinchoninic acid (BCA) protein assay kit (Thermo Fisher Scientific, Inc.) according to the manufacturer's instructions. A total of 10-20 μg of proteins were separated on a 10% SDS-polyacrylamide gel and electrophoretically transferred to PVDF membranes (EMD Millipore). The membranes were incubated with one of the following primary antibodies: TF (1:1,000; cat. no. 55147S, Cell Signaling Technology, Inc.), GAPDH (1:2,000; cat. no. sc-32233; Santa Cruz Biotechnology, Inc.), Flotillin-1 (1:200; cat. no. sc25506; Santa Cruz Biotechnology, Inc.), GM130 (1:250; cat. no. 610822, BD Biosciences), Lamin A/C (1:500; cat. no. sc-7292; Santa Cruz Biotechnology, Inc.) and Tom20 (1:500; cat. no. sc-17764, Santa Cruz Biotechnology, Inc.) at 4˚C overnight and were then incubated with HRP-conjugated goat-anti-rabbit (1:2,000; cat. no. sc-2004, Santa Cruz Biotechnology, Inc.) or mouse (1:4,000 for GAPDH or 1:2,000 for the rest, cat. no. sc-2005; Santa Cruz Biotechnology, Inc.) IgG secondary antibodies at room temperature for 2 h. The membranes were visualized using an enhanced-chemiluminescence system (Thermo Fisher Scientific, Inc.). The bands were quantified using Image J 1.52a software. The expression level of TF was normalized to that of GAPDH.

EdU incorporation assay. Proliferating HUVECs were identified using the Click-iT Plus EdU Imaging kit (Life technologies; Thermo Fisher Scientific, Inc.). Following co-culture with exosomes or transfection with miRNA inhibitor, the HUVECs were incubated with 10 μM EdU for 16 h, fixed with 4% paraformaldehyde for 15 min at room temperature and washed with PBS containing 3% bovine serum albumin (BSA). The cells were then treated according to the following steps: 20 min in 0.5% Triton X-100, 30 min in the Click-iT Plus reaction cocktail, and 30 min in 5 μg/ml of Hoechst 33342 at room temperature. Cell images were captured using an Olympus IX70 microscope (Olympus Corporation). The ratio of EdU-positive cells to total cells was analyzed by counting approximately 1,000 cells in several randomly selected fields.

Scratch wound migration assay. The assessment of HUVEC migration was performed as previously described (23). A confluent layer of HUVECs in 24-well plates was scratched with a sterile 10-μl tip and the detached cells were removed by washing with PBS. The adherent cells were then incubated with 5 μg/ml exosomes for 20 h before cell migration was captured using a Leica DM IL LED microscope (Leica Microsystems GmbH) and quantified by measuring the size of recovered area using ImageJ 1.52a software.

Tube formation assay. Matrigel Matrix Growth Factor Reduced (BD Biosciences) (300 μl/well) was coated on 24-well plates and incubated at 37˚C for 30 min. Approximately 8x10^4 HUVECs/well were then seeded onto the gel and cultured in FBS-free ECM for 20 h to allow tube formation. Tube formation was observed using a Leica DM IL LED microscope (Leica Microsystems GmbH). The averages of the total number of branching points and total number of loops in 4 representative fields were analyzed using ImageJ 1.52a software.

In vivo Matrigel plug assay. A total of 8 female, 8-week-old, BALB/c nude mice (Charles River Laboratories, Inc.) were used in this study. All the mice were housed in specific pathogen-free conditions under a controlled temperature (23±3˚C), humidity (60±15%) and 12 h dark/light cycle, with sterile rodent chow and water provided *ad libitum*. The mice were kept in specific pathogen-free grade filter-top cages and infectious diseases were not detected. Following transfection with miR-92a-3p inhibitor or NC inhibitor for 48 h, the HUVECs were mixed with Matrigel Matrix High Concentration (BD Biosciences) at ratio of 1:1 (V:V). Subsequently, 1 ml of mixture containing 1x10^7 HUVECs was subcutaneously injected into the dorsal surface of each nude mouse (n=4/group) using a 25-gauge needle. After 2 weeks, the mice were euthanized by an intraperitoneal injection of an overdose of pentobarbital (120 mg/kg). The Matrigel plugs were harvested, transferred to ice-cold PBS and embedded in OCT compound. Serial 5-μm-thick sections were cut and stained with anti-CD31 antibody (1:100; cat. no. ab28364, Abcam) at 4˚C overnight. The sections were observed under a Jenoptik fluorescence microscope. A representative surface of blood vessels was analyzed by analyzing the CD31-positive region (24). The animal experimental protocol was approved by Peking University People's Hospital Ethics Committee (approval no. 2016PHC072).

Luciferase reporter assay. Luciferase reporter assay was performed as previously described (21). The sequence (1,284 bp) of TF 3'UTR containing the miR-92a-3p binding site was synthesized and cloned into a Firefly luciferase reporter plasmid pMIR-REPORT™ (Ambion; Thermo Fisher Scientific, Inc.). To construct the mutant plasmid, the predicted target nucleotides of miR-92a-3p in TF 3'UTR were changed to opposite bases. 293 cells were co-transfected with 0.06 pmol/μl of miRNA mimic, 0.3 ng/μl of Firefly luciferase reporter plasmid, as well as 0.01 ng/μl of *Renilla* luciferase as the control (pRLTK; Promega Corporation). Following 24 h of transfection, the luciferase activity was measured using the Dual Luciferase Assay System (Promega Corporation). Each measured value of Firefly luciferase activity was normalized to that of *Renilla* luciferase activity.

Statistical analysis. The data are presented as the means ± standard error of the mean (SEM). The Student's t-test was used to compare differences between 2 groups, and one-way ANOVA followed by Tukey's post hoc test was used to compare differences among multiple groups. A two-sided value of $P<0.05$ was considered to indicate a statistically significant difference. Prism 5.0 was used for all statistical analyses.

Results

Characterization and internalization of exosomes derived from ECs. To obtain exosomes from oxidative stress-stimulated ECs, HUVECs were cultured in ECM containing 5% of exosome-free FBS and treated with 100 μM of H_2O_2 (these exosomes were termed Exo$^{-H_2O_2}$). The control exosomes were obtained from HUVECs without H_2O_2 stimulation (these exosomes were termed Exo^{-Con}). Following 24 h of incubation, the conditioned medium was collected and the exosomes were isolated. The results of NTA revealed that the particle size distribution of the exosomes was 50-140 nm in both groups (Fig. 1A); TEM analysis revealed the cup-shaped appearance of the exosomes (Fig. 1B). The results of western blot analysis demonstrated that the exosomes (marker, flotillin 1) (10,25) were not contaminated with Golgi (marker, GM130), nuclear (marker, Lamin A/C) and mitochondrial (marker, Tom20) substances (Fig. 1C).

To examine the uptake of exosomes by recipient ECs, exosomes were labeled with PKH26 and incubated with HUVECs. Confocal laser scanning microscopic analysis revealed that the PKH26-labled exosomes were efficiently internalized by the HUVECs (Fig. 1D).

Oxidative stress-induced ECs promote EC proliferation, migration and angiogenesis. EdU incorporation assay, scratch wound migration assay and tube formation assay were performed to examine the effects of exosomes released by oxidative stress-stimulated ECs on the proliferation, migration and angiogenesis of recipient ECs, respectively. For the EdU incorporation assay, the HUVECs were incubated with 5 μg/ml exosomes (Exo$^{-H_2O_2}$ or Exo^{-Con}). Following 48 h of incubation, HUVECs were treated with 10 μM EdU for 16 h. The proliferating cells were incorporated with EdU (green) and nuclei were stained with Hoechst 33342 (blue). HUVEC proliferation was increased by 1.2-fold by Exo$^{-H_2O_2}$ compared with that by Exo^{-Con} (Fig. 2A and B). For scratch wound migration assay, the HUVECs were scratched and incubated with exosomes for 20 h. HUVEC migration was enhanced by 1.5-fold by Exo$^{-H_2O_2}$ compared with that by Exo^{-Con} (Fig. 2C and D). For tube formation assay, the HUVECs were treated with exosomes for 24 h and then seeded in the Matrigel, and endothelial networks could be observed after 20 h. The numbers of total branching points and loops increased by 1.3- and 1.6-fold, respectively, as compared to the control (Fig. 2E-G).

miR-92a-3p expression is inhibited by Exo$^{-H_2O_2}$ in recipient ECs. To explore whether miRNAs mediate the effects of Exo$^{-H_2O_2}$ on recipient ECs, miRNAs differentially expressed in Exo$^{-H_2O_2}$- and Exo^{-Con}-treated HUVECs were identified by small RNA sequencing. Following 24 h of incubation with exosomes, total RNA was extracted from the HUVECs. The

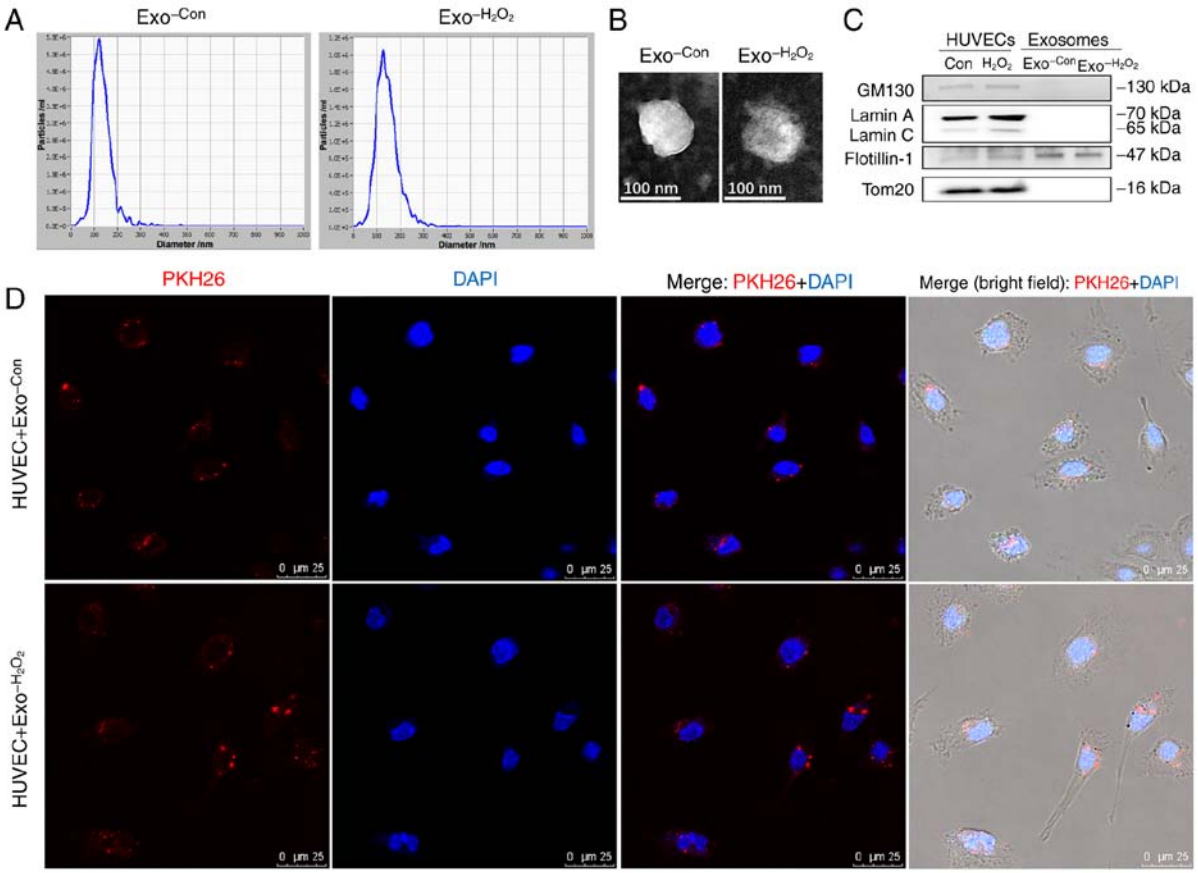

Figure 1. Characterization and internalization of exosomes derived from HUVECs. (A) Particle size distribution of endothelial exosomes measured by nanoparticle tracking analysis. The size of most particles was 50-140 nm. (B) The appearance of exosomes analyzed by a transmission electron microscope. Bars, 100 nm. (C) The purity of exosomes assessed by western blot analysis for exosomes (Flotillin 1), nuclear (Lamin A/C), mitochondrial (Tom20) and Golgi (GM130) marker proteins. (D) The uptake of PKH26-labeled exosomes by HUVECs observed using confocal laser scanning microscopy (PKH26 in red, DAPI in blue). Bars, 75 μm. Exo^{-Con}, exosomes derived from HUVECs without H_2O_2 stimulation; Exo$^{-H_2O_2}$, exosomes derived from HUVECs stimulated with H_2O_2 for 24 h; HUVECs, human umbilical vein endothelial cells.

results indicated the presence of 12 miRNAs differentially expressed between the 2 groups (Fig. 3A and Table SI). Among the 12 miRNAs, miR-92a-3p was the most abundant and has been reported to play a key role in regulating angiogenesis (13). Therefore, miR-92a-3p was selected for further validation by RT-qPCR. The results revealed that miR-92a-3p expression was decreased by 40% in the Exo$^{-H_2O_2}$-treated HUVECs compared with that in the Exo^{-Con}-treated group (Fig. 3B). Furthermore, to reveal the cause for the decrease in miR-92a-3p expression in recipient HUVECs, the expression of primary miR-92a (pri-miR-92a-1 and pri-miR-92a-2) in HUVECs co-cultured with exosomes was detected by RT-PCR. The results revealed that pri-miR-92a-1 expression was decreased by 20% (Fig. 3C) in the Exo$^{-H_2O_2}$-treated HUVECs compared with that in the control, and pri-miR-92a-2 was almost undetectable (data not shown) in both groups. Taken together, these results suggested that the Exo$^{-H_2O_2}$-mediated stimulation of EC proliferation, migration and angiogenesis may be achieved via the inhibition of miR-92a-3p in recipient cells.

miR-92a-3p overexpression blocks the effects of Exo$^{-H_2O_2}$ on recipient ECs. To investigate whether miR-92a-3p is involved in the effects of Exo$^{-H_2O_2}$ on target ECs, miR-92a-3p expression was increased by transfecting the cells with miR-92a-3p mimic (miR-92a-3p-m) for 24 h prior to the addition of exosomes. The results of RT-qPCR revealed that miR-92a-3p expression was significantly upregulated (Fig. 4H). EdU incorporation assay, scratch wound migration assay and tube formation assay were performed after incubating the HUVECs with exosomes for 24 h. Compared with Exo^{-Con} (group, NC-m + Exo^{-Con}) (set as 1), Exo$^{-H_2O_2}$ (group, NC-m + Exo$^{-H_2O_2}$) promoted HUVEC proliferation (1.3-fold) (Fig. 4A and B), migration (1.6-fold) (Fig. 4C and D) and angiogenic capacity (total branching points, 1.6-fold; number of loops, 2.5-fold) (Fig. 4E-G). The above-mentioned effects induced by Exo$^{-H_2O_2}$ were all abrogated by the overexpression of miR-92a-3p (group, miR-92a-3p-m + Exo$^{-H_2O_2}$) (Fig. 4A-G). These results indicated that downregulated expression of miR-92a-3p mediated the role of Exo$^{-H_2O_2}$ in promoting endothelial proliferation, migration and angiogenesis.

Inhibition of miR-92a-3p induces angiogenesis. To further determine the role of miR-92a-3p in angiogenesis, miR-92a-3p expression was directly inhibited by transfecting the HUVECs with miR-92a-3p inhibitor for 48 h. The decreased expression of miR-92a-3p induced EC proliferation (1.2-fold) (Fig. S1A and B), migration (2.0-fold) (Fig. S1C and D) and angiogenesis *in vitro* (total branching points, 1.7-fold; number of loops, 2.8-fold) (Fig. 5A-C).

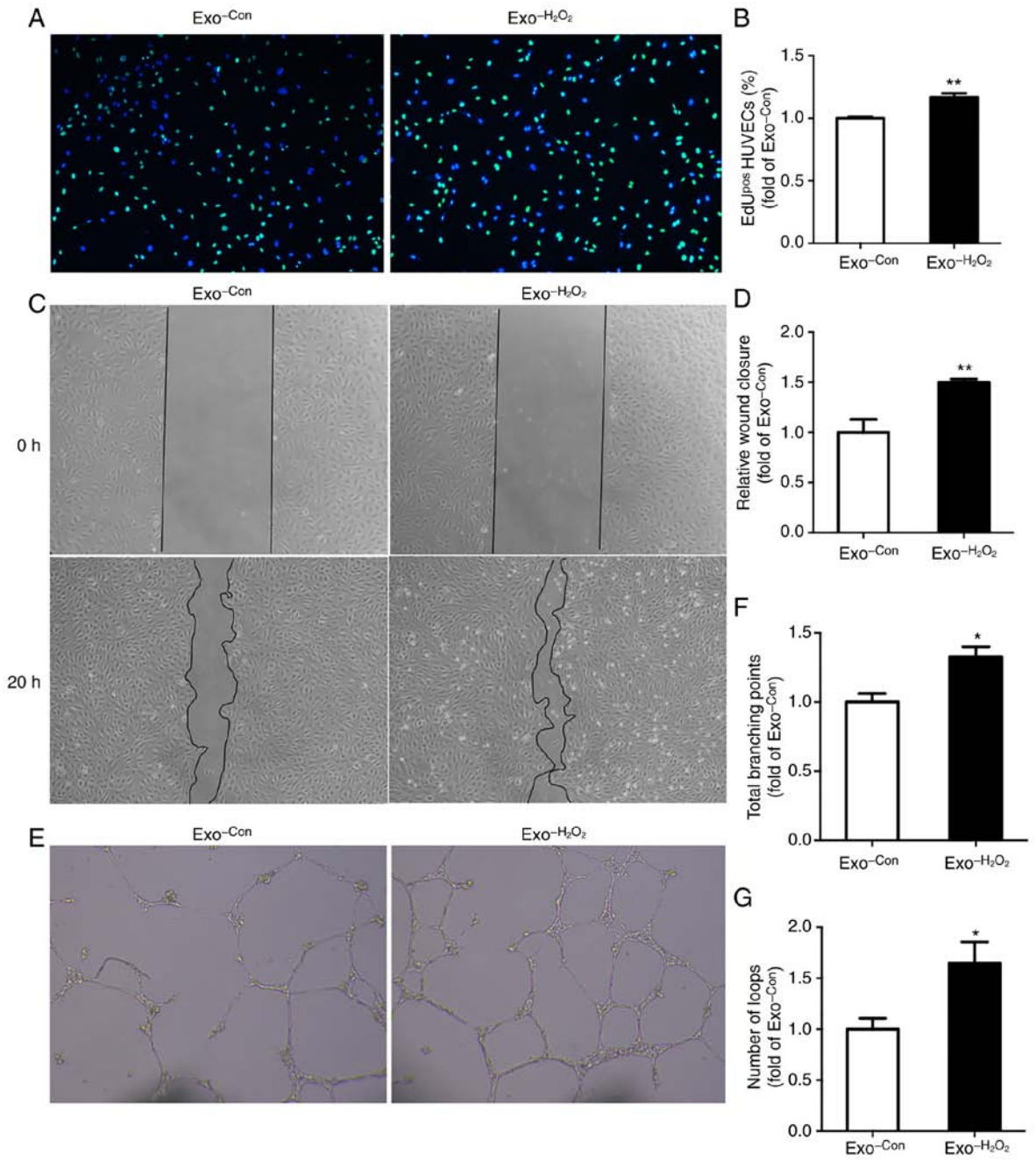

Figure 2. Effects of exosomes on HUVEC proliferation, migration and angiogenesis. HUVECs were incubated in FBS-free medium containing 5 μg/ml $Exo^{-H_2O_2}$ or Exo^{-Con}. (A) HUVEC proliferation was measured by EdU incorporation assay and (B) quantified by counting the percentage of EdU-positive cells in total cells. Proliferating cells were incorporated with EdU (green) and nuclei were stained with Hoechst 33342 (blue); n=3. (C) Cell migration was assessed by scratch wound migration assay and (D) quantified by measuring the scratch closure area; n=4. (E) *In vitro* angiogenesis was analyzed by tube formation assay and quantified by measuring the total number of (F) branching points and (G) loops; n=3. Magnification, x100. *P<0.05, **P<0.01 vs. Exo^{-Con}. Exo^{-Con}, exosomes derived from HUVECs without H_2O_2 stimulation; $Exo^{-H_2O_2}$, exosomes derived from HUVECs stimulated with H_2O_2 for 24 h; HUVECs, human umbilical vein endothelial cells.

Moreover, the *in vivo* Matrigel plug assay revealed that *in vivo* blood vessel formation was enhanced by 1.5-fold in the miR-92a-3p inhibitor group (Fig. 5D-F). Taken together, these results further indicated that $Exo^{-H_2O_2}$ promoted angiogenesis by decreasing miR-92a-3p expression in recipient HUVECs.

miR-92a-3p inhibits TF expression in ECs. To identify the targets of miR-92a-3p involved in angiogenesis, differentially expressed genes were identified in HUVECs transfected for 48 h with miR-92a-3p inhibitor or NC-inhibitor. The results identified 197 differentially expressed mRNAs, among which 91 mRNAs were upregulated (Fig. S2). In addition, 4,167 targets of miR-92a-3p were predicted using the RNAhybrid program (26), including 21 upregulated genes that were also identified by mRNA sequencing (Fig. S2 and Table I). Among the genes closely related to angiogenesis, TF (F3) was most significantly upregulated.

To determine whether TF is a novel target of miR-92a-3p, gain- and loss-of-function experiments were performed by

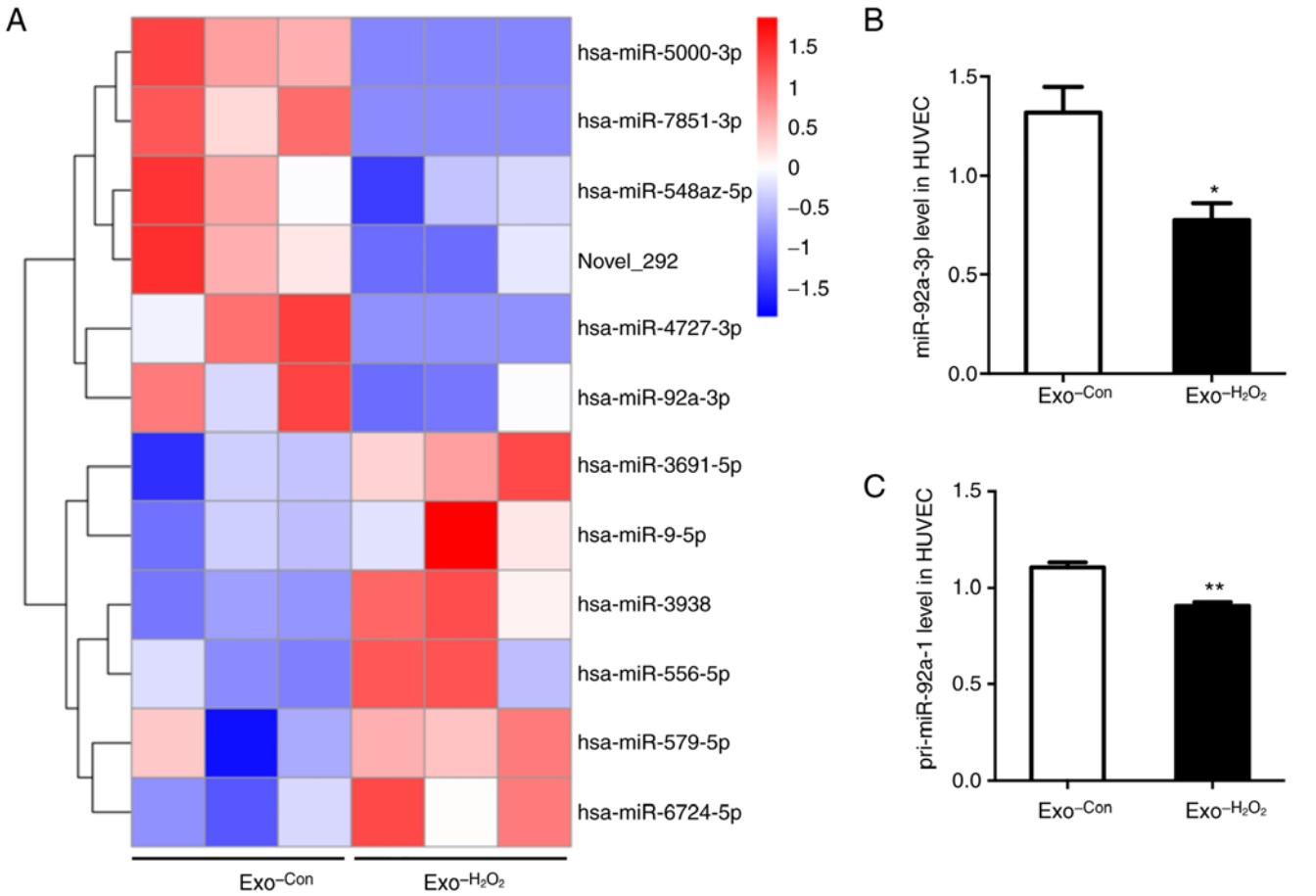

Figure 3. Differentially expressed miRNAs in HUVECs treated with $Exo^{-H_2O_2}$ and Exo^{-Con}. (A) miRNA expression profiles were analyzed by small RNA sequencing and the cluster analysis of differentially expressed miRNAs between the 2 groups was illustrated with a heatmap. Color intensity was scaled within each row and the highest expression value corresponds to light red, while the lowest expression value corresponds to dark blue. miR-92a-3p was the most abundant one among the 12 differentially expressed miRNAs; n=3. (B) miR-92a-3p and (C) pri-miR-92a-1 expression levels were determined by RT-qPCR. RNU6B (for miR-92a-3p) and GAPDH (for pri-miR-92a-1) were used as the controls for normalization. $^{*}P<0.05$, $^{**}P<0.01$ vs. Exo^{-Con}; n=3. Exo^{-Con}, exosomes derived from HUVECs without H_2O_2 stimulation; $Exo^{-H_2O_2}$, exosomes derived from HUVECs stimulated with H_2O_2 for 24 h; HUVECs, human umbilical vein endothelial cells.

transfecting HUVECs for 48 h with miR-92a-3p mimic or inhibitor, respectively. The results of RT-qPCR revealed that miR-92a-3p was successfully overexpressed (Fig. 6A) or inhibited (Fig. 6C). Accordingly, the upregulation of miR-92a-3p inhibited TF expression by 30% at the mRNA level (Fig. 6A) and by 33% at the protein level (Fig. 6B), whereas the downregulation of miR-92a-3p increased TF expression by 6.4-fold at the mRNA level (Fig. 6C) and by 1.6-fold at the protein level (Fig. 6D).

TF is a direct target of miR-92a-3p. To examine whether miR-92a-3p acts directly on TF 3'UTR, 2 luciferase reporter plasmids containing wild-type (TF-luci-WT) or mutant TF 3'UTR (TF-luci-MUT) (Fig. 6E) were constructed. The results of luciferase activity assay revealed that miR-92a-3p inhibited the luciferase activity of TF-luci-WT constructs by approximately 20% (Fig. 6F), but failed to decrease the luciferase activity of TF-luci-MUT (Fig. 6F).

Taken together, the present study revealed a novel proangiogenic mechanism between ECs mediated by oxidative stress-stimulated endothelial exosomes by inhibiting the expression of miR-92a-3p in target ECs (Fig. 7).

Discussion

Various types of pathological stimulation can lead to vascular endothelial activation and injury. Activated or injured ECs release characteristic extracellular vesicles (EVs), including exosomes, microvesicles and apoptotic bodies. The content of exosomes may partly depend on the stimuli and the state of donor cells, which can exert distinct biological effects on target cells (4). The roles of non-EC-derived EVs in angiogenesis have previously been investigated (3), whereas the regulation of endothelial exosomes in angiogenesis remains to be fully determined.

The present study aimed to investigate the role of exosomes shed by oxidative stress-activated ECs in angiogenesis. It was found that the exosomes derived from oxidative stress-activated ECs promoted EC proliferation, migration and angiogenesis, which were mediated by the downregulation of miR-92a-3p in recipient ECs. Moreover, TF, a procoagulant and proangiogenic gene (27), was identified as a novel target of miR-92a-3p, and may be involved in the role of activated endothelial exosomes in promoting angiogenesis.

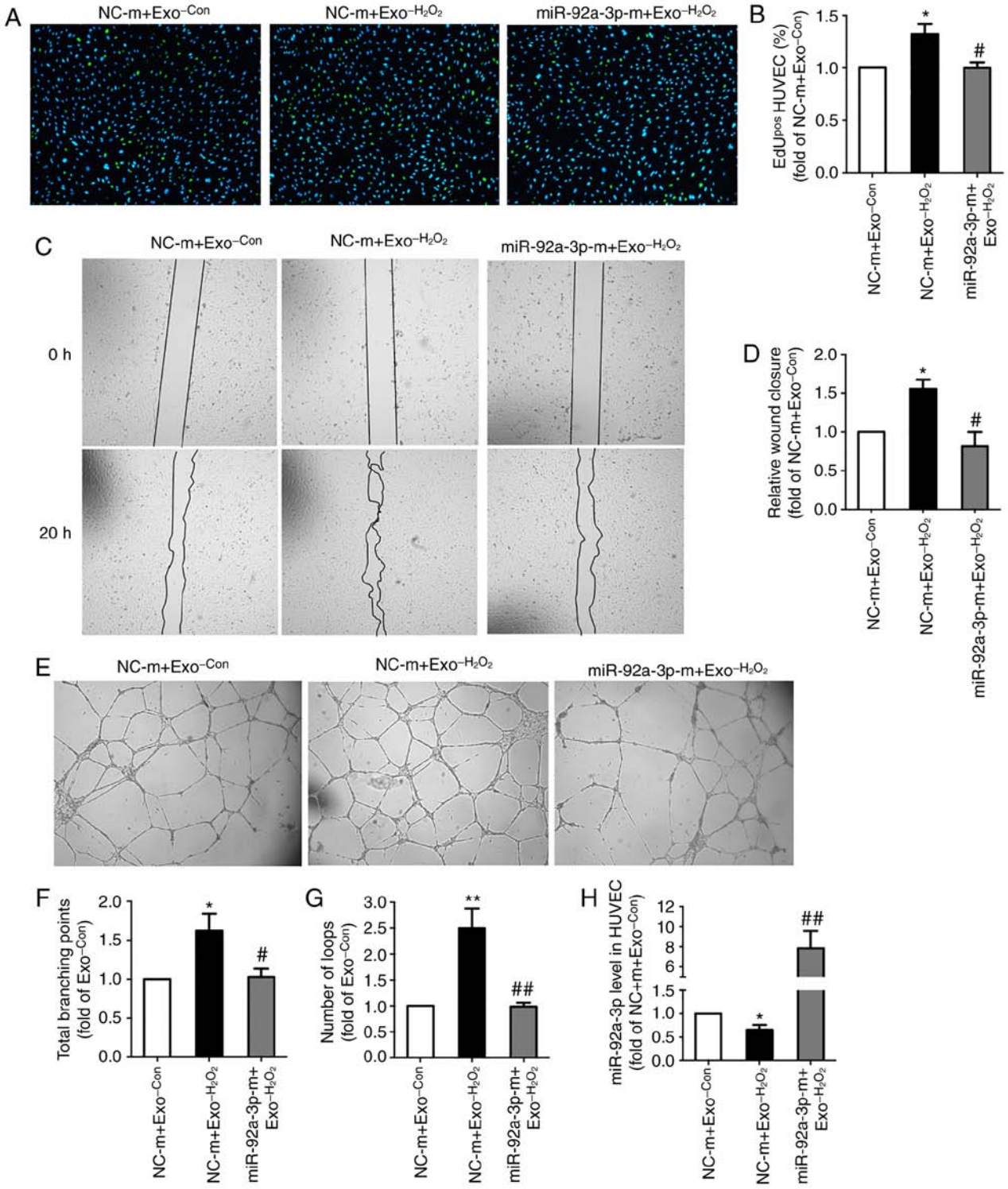

Figure 4. Blocking effects of upregulated miR-92a-3p on Exo$^{-H_2O_2}$-stimulated HUVEC proliferation, migration and angiogenesis. HUVECs were incubated in FBS-free medium containing 5 μg/ml Exo$^{-H_2O_2}$ or Exo^{-Con} following the addition of miR-92a-3p mimic (miR-92a-3p-m) or NC mimic (NC-m). (A) Cell proliferation was determined by EdU incorporation assay and (B) quantified by counting the percentage of EdU-positive cells in total cells; n=3. (C) Cell migration was assessed by scratch wound assay and (D) quantified by measuring the scratch closure area; n=3. (E) *In vitro* angiogenesis was analyzed by tube formation assay and quantified by measuring the total number of (F) branching points and (G) loops; n=4. (H) The miR-92a-3p level in HUVEC was detected by RT-qPCR; n=3. Magnification, x100. *P<0.05, **P<0.01 vs. NC-m + Exo^{-Con}; $^{\#}$P<0.05, $^{\#\#}$P<0.01 vs. NC-m + Exo$^{-H_2O_2}$. Exo^{-Con}, exosomes derived from HUVECs without H_2O_2 stimulation; Exo$^{-H_2O_2}$, exosomes derived from HUVECs stimulated with H_2O_2 for 24 h; HUVECs, human umbilical vein endothelial cells.

Several studies have revealed the signaling transfer and proangiogenic effects of exosomes between non-ECs and ECs (5-9). As regards EC-to-EC communication, it has been reported that exosomes isolated from ECs cultured in exosome-free medium or stimulated by interleukin-3 can promote angiogenesis (10,11). Similarly, it was observed in the present study that H_2O_2-activated endothelial exosomes were effectively taken up by target ECs and led to an

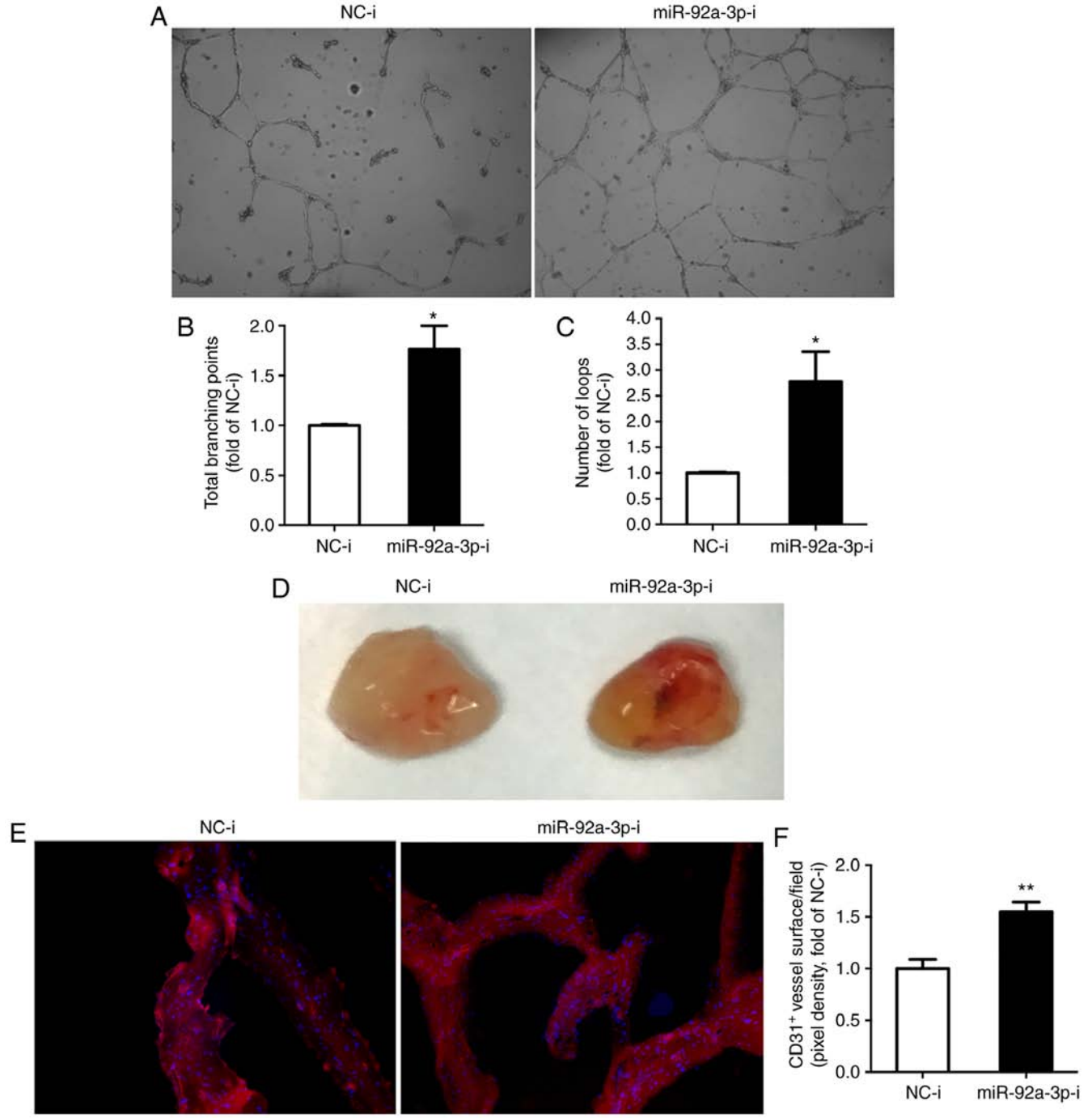

Figure 5. Effects of the downregulation of miR-92a-3p on *in vitro* and *in vivo* angiogenesis. HUVECs were transfected with miR-92a-3p inhibitor (miR-92a-3p-i) or NC inhibitor (NC-i) for 48 h. (A) *In vitro* angiogenesis was analyzed by tube formation assay and quantified by measuring the total number of (B) branching points and (C) loops. *P<0.05 vs. NC-I; n=3. (D) *In vivo* angiogenesis was assessed by Matrigel plug assay and the gross look of Matrigel plugs is shown. (E) Neovessels in Matrigel plugs were assessed by immunofluorescence staining of CD31, and (F) quantified by analyzing CD31-positive surface area of blood vessels in each field. **P<0.01 vs. NC-I; n=4/group. HUVECs, human umbilical vein endothelial cells.

enhanced cell proliferation, migration and angiogenesis. Although the exosomes isolated from ECs exposed to different stimuli and in a different state exerted similar effects, the mechanisms reported in these studies differ. The exosomes isolated from ECs cultured in an exosome-free medium promoted angiogenesis by suppressing the expression of ataxia telangiectasia mutated (ATM) via transferring miR-214 into recipient ECs. Endothelial exosomes generated in response to interleukin-3 stimulation enhanced angiogenesis by delivering miR-126-3p and pSTAT5 into recipient ECs, leading to the activation of the pro-angiogenic pathway and the suppression of antiangiogenic signal molecules (10,11). Herein, it was confirmed that the exosomes isolated from H_2O_2-activated ECs stimulated angiogenesis by decreasing miR-92a-3p expression in recipient cells. The effect was similar to that observed with the direct inhibition of miR-92a-3p in ECs observed in the present study and other studies (14-18). Conversely, a recent study reported that endothelial microvesicles (100-1,000 nm in size), which were derived from ECs exposed to oxidized low-density

Table I. Potential targets of miR-92a-3p in HUVECs.

Gene	Fold change (miR-92a-3p-i vs. NC-i)	FDR
TNFRSF9	3.5	4.1E-05
NCOA7	1.9	5.5E-11
TNFAIP2	3.7	0.0E+00
IL1R1	1.6	1.2E-02
NUAK2	2.3	8.2E-13
INSR	1.6	2.2E-04
GUCY1A3	2.7	4.9E-11
F3 (TF)	7.0	0.0E+00
AQP1	1.8	1.5E-04
C2CD4A	13.0	0.0E+00
SOD2	2.0	1.3E-12
SLC16A7	2.0	4.0E-03
SPAST	1.6	1.3E-03
SGPP2	11.6	2.8E-05
CX3CL1	6.7	0.0E+00
TRAF1	1.6	5.5E-03
TNIP3	4.9	3.4E-09
C8orf4	2.2	2.7E-12
ZC2HC1A	2.3	1.5E-02
ICAM1	2.5	1.2E-15
CD83	2.1	2.8E-04

Predicted target genes of miR-92a-3p with a fold change of >1.5 and FDR of <0.05 are shown. FDR, false discovery rate; miR-92a-3p-i, miR-92a-3p inhibitor; NC-i, NC inhibitor; HUVECs, human umbilical vein endothelial cells.

lipoprotein (oxLDL) stimulation, promoted angiogenesis by transferring upregulated miR-92a-3p to recipient cells (19). The controversial role of miR-92a-3p in regulating angiogenesis may change depending on the experimental model and condition.

In previous findings on cell-to-cell communications, the dysregulation of miRNAs in recipient cells has been found to be usually caused by the delivery of miRNAs from donor cells. In addition, intercellular protein transfer can regulate the activity of specific signal pathways in recipient cells (28). In the present study, it was found that the decreased expression of miR-92a-3p in Exo$^{-H_2O_2}$-treated HUVEC may be attributed to the transcriptional inhibition of miR-92a-3p, which may be caused by the cargo in exosomes. The potential active molecules or signaling pathways involved in this process warrant further investigation. miR-9-5p has also been reported to be closely associated with angiogenesis (29-32). In the small RNA sequencing data of the present study, miR-9-5p was significantly upregulated in Exo$^{-H_2O_2}$-treated HUVECs. It was also found that miR-9-5p expression was increased in both H_2O_2-stimulated HUVEC and their exosomes (data not shown). These results suggested that miR-9-5p, delivered by Exo$^{-H_2O_2}$-induced ECs, may also be involved in the regulation of the biological effects on target HUVECs, and the molecular mechanisms of miR-9-5p upregulation differ from those of miR-92a-3p downregulation in HUVECs caused by Exo$^{-H_2O_2}$ exposure. miR-9-5p and miR-92a-3p may synergistically regulate EC angiogenesis induced by Exo$^{-H_2O_2}$, and this hypothesis is still under investigation.

There are multiple known mRNA targets of miR-92a in regulating cell proliferation, migration and angiogenesis, such as Kruppel-like factor 2 (KLF2) (33), KLF4 (15), integrin subunit alpha5 (ITGA5) (14,17) and sirtuin 1 (17). The mRNA expression profiles obtained in the present study suggested that 91 of 197 differently expressed genes were markedly upregulated by the inhibition of miR-92a-3p in target ECs. A to9tal of 21 of the 91 genes were candidate targets of miR-92a-3p predicted by the RNAhybrid program. Among these 21 genes, TF is not only an initiator of blood coagulation, but also an activator of angiogenesis, and may mediate the effects of miR-92a-3p observed in the present study. There are 2 natural isoforms of TF, membrane-bound full-length (fl)TF and soluble alternatively spliced (as)TF. Both isoforms have been found to affect cell proliferation, migration and angiogenesis (27). It has been reported that the inhibition of miR-19a and miR-126 promoted flTF and asTF synthesis in EC (34). flTF has been shown to indirectly promote angiogenesis via the induction of proangiogenic factor expression by the FVIIa/protease-activated receptors (PAR)-2 dependent signaling (35), whereas asTF has been reported to directly increase the proangiogenic activity of EC independently of the PAR-2 signaling via integrin ligation (36). In the present study, TF was found as a new target of miR-92a-3p by gain and loss of function assays and luciferase reporter assays.

There are some limitations to the present study. The present study did not i) validate the pro-angiogenic effect of oxidative stress-activated endothelial exosomes through *in vivo* experiments; ii) determine the molecules or signaling pathway, inducing the downregulation of miR-92a-3p in target EC incubated with oxidative stress-activated endothelial exosomes; iii) clarify the synergistically proangiogenic role of miR-9-5p from oxidative stress-activated endothelial exosomes and miR-92a-3p in target ECs. These questions remain to be investigated in future studies.

In conclusion, the findings of the present study provide new mechanistic insight into the regulation of angiogenesis. In response to oxidative stress, exosomes are released from ECs and convey potentially proangiogenic signals to target ECs, eventually leading to a decreased miR-92a-3p expression and subsequent angiogenesis. Moreover, TF may mediate the biological effects of miR-92a-3p on ECs. Finally, this study revealed a pro-angiogenic mechanism in ECs mediated by the suppression of miR-92a-3p expression via oxidative stress-stimulated endothelial exosomes (Fig. 7).

Acknowledgements

Not applicable.

Funding

The present study was funded by grants from the National Natural Science Foundation of China (nos. 81600340, 81770356 and 81970301), Capital Health Research and

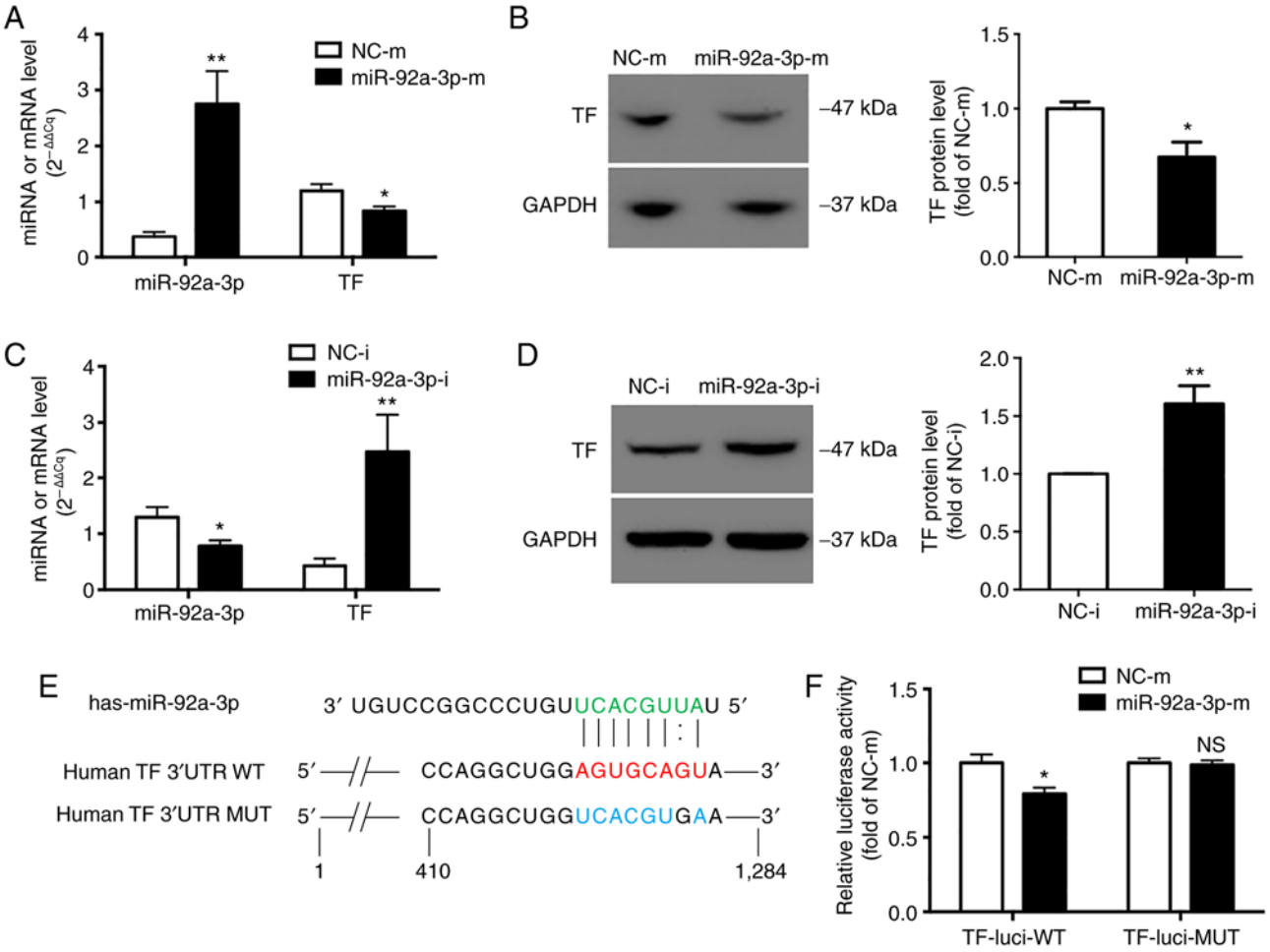

Figure 6. Regulatory effects of miR-92a-3p on TF expression in HUVECs. HUVECs were transfected with miR-92a-3p mimic (miR-92a-3p-m), NC mimic (NC-m), miR-92a-3p inhibitor (miR-92a-3p-i) or NC inhibitor (NC-i) for 48 h. (A and C) The levels of miR-92a-3p and TF mRNA were measured by RT-qPCR and normalized to RNU6B (for miR-92a-3p) or GAPDH (for TF); n=3. (B and D) The TF protein level was detected by western blot analysis with GAPDH as a loading control; n=4. (E) The putative binding sites of miR-92a-3p in the human TF 3'UTR. Seed sequences of miR-92a-3p are shown in green. Binding sites of miR-92a-3p to TF 3'UTR are shown in red and mutated sites were shown in blue. TF-luci-WT plasmid contained wild-type TF 3'UTR sequences while TF-luci-MUT plasmid carried mutated TF 3'UTR sequences. (F) 293 cells were transfected with TF-luci-WT or TF-luci-MUT, along with miR-92a-3p mimic (miR-92a-3p-m) or NC mimic (NC-m) for 24 h. Luciferase activity assays were performed and the Firefly luciferase activities were normalized to *Renilla* luciferase activities in each group; n=4. *P<0.05, **P<0.01 vs. respective control. 3'UTR, 3' untranslated region; NS, no significance; HUVECs, human umbilical vein endothelial cells; TF, tissue factor.

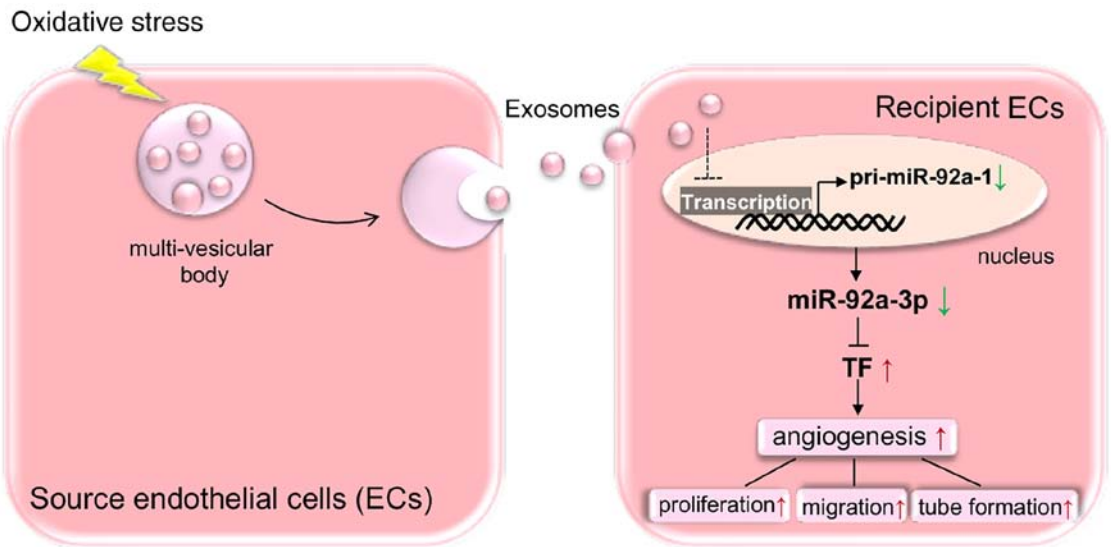

Figure 7. Proposed mechanisms. Exosomes released from oxidative stress-stimulated EC were endocytosed by adjacent ECs to suppress miR-92a-3p expression in recipient cells. Inhibition of miR-92a-3p upregulated TF and promoted EC migration, proliferation and angiogenesis. EC, endothelial cells; TF, tissue factor.

Development of Special Funds (no. 2020-2-4084) and Peking University People's Hospital Research and Development Funds (no. RDY2018-26).

Availability of data and materials

The datasets used and/or analyzed in the current study are available from the corresponding author upon reasonable request.

Authors' contributions

HC and SL designed the study. SL performed experiments, analyzed data and wrote the manuscript. LY performed experiments and analyzed data. LS, ZL, CL, FZ, YC and MW performed experiments. HC and CL critically revised the manuscript. All authors read and approved the final manuscript.

Ethics approval and consent to participate

The animal experimental protocol was approved by Peking University People's Hospital Ethics Committee (approval no. 2016PHC072).

Patient consent for publication

Not applicable.

Competing interests

The authors declare that they have no competing interests.

References

1. Potente M and Mäkinen T: Vascular heterogeneity and specialization in development and disease. Nat Rev Mol Cell Biol 18: 477-494, 2017.
2. Münzel T, Camici GG, Maack C, Bonetti NR, Fuster V and Kovacic JC: Impact of oxidative stress on the heart and vasculature: Part 2 of a 3-part series. J Am Coll Cardiol 70: 212-229, 2017.
3. Todorova D, Simoncini S, Lacroix R, Sabatier F and Dignat-George F: Extracellular vesicles in angiogenesis. Circ Res 120: 1658-1673, 2017.
4. Mathieu M, Martin-Jaular L, Lavieu G and Théry C: Specificities of secretion and uptake of exosomes and other extracellular vesicles for cell-to-cell communication. Nat Cell Biol 21: 9-17, 2019.
5. Li J, Zhang Y, Liu Y, Dai X, Li W, Cai X, Yin Y, Wang Q, Xue Y, Wang C, *et al*: Microvesicle-mediated transfer of microRNA-150 from monocytes to endothelial cells promotes angiogenesis. J Biol Chem 288: 23586-23596, 2013.
6. Zheng B, Yin WN, Suzuki T, Zhang XH, Zhang Y, Song LL, Jin LS, Zhan H, Zhang H, Li JS and Wen JK: Exosome-mediated miR-155 transfer from smooth muscle cells to endothelial cells induces endothelial injury and promotes atherosclerosis. Mol Ther 25: 1279-1294, 2017.
7. Deregibus MC, Cantaluppi V, Calogero R, Lo Iacono M, Tetta C, Biancone L, Bruno S, Bussolati B and Camussi G: Endothelial progenitor cell derived microvesicles activate an angiogenic program in endothelial cells by a horizontal transfer of mRNA. Blood 110: 2440-2448, 2007.
8. Gong M, Yu B, Wang J, Wang Y, Liu M, Paul C, Millard RW, Xiao DS, Ashraf M and Xu M: Mesenchymal stem cells release exosomes that transfer miRNAs to endothelial cells and promote angiogenesis. Oncotarget 8: 45200-45212, 2017.
9. Umezu T, Tadokoro H, Azuma K, Yoshizawa S, Ohyashiki K and Ohyashiki JH: Exosomal miR-135b shed from hypoxic multiple myeloma cells enhances angiogenesis by targeting factor-inhibiting HIF-1. Blood 124: 3748-3757, 2014.
10. van Balkom BW, de Jong OG, Smits M, Brummelman J, den Ouden K, de Bree PM, van Eijndhoven MA, Pegtel DM, Stoorvogel W, Würdinger T and Verhaar MC: Endothelial cells require miR-214 to secrete exosomes that suppress senescence and induce angiogenesis in human and mouse endothelial cells. Blood 121: 3997-4006, 2013.
11. Lombardo G, Dentelli P, Togliatto G, Rosso A, Gili M, Gallo S, Deregibus MC, Camussi G and Brizzi MF: Activated Stat5 trafficking via endothelial cell-derived extracellular vesicles controls IL-3 pro-angiogenic paracrine action. Sci Rep 6: 25689, 2016.
12. Kim YW and Byzova TV: Oxidative stress in angiogenesis and vascular disease. Blood 123: 625-631, 2014.
13. Sun LL, Li WD, Lei FR and Li XQ: The regulatory role of microRNAs in angiogenesis-related diseases. J Cell Mol Med 22: 4568-4587, 2018.
14. Bonauer A, Carmona G, Iwasaki M, Mione M, Koyanagi M, Fischer A, Burchfield J, Fox H, Doebele C, Ohtani K, *et al*: MicroRNA-92a controls angiogenesis and functional recovery of ischemic tissues in mice. Science 324: 1710-1713, 2009.
15. Iaconetti C, Polimeni A, Sorrentino S, Sabatino J, Pironti G, Esposito G, Curcio A and Indolfi C: Inhibition of miR-92a increases endothelial proliferation and migration in vitro as well as reduces neointimal proliferation in vivo after vascular injury. Basic Res Cardiol 107: 296, 2012.
16. Hinkel R, Penzkofer D, Zühlke S, Fischer A, Husada W, Xu QF, Baloch E, van Rooij E, Zeiher AM, Kupatt C and Dimmeler S: Inhibition of microRNA-92a protects against ischemia/reperfusion injury in a large-animal model. Circulation 128: 1066-1075, 2013.
17. Daniel JM, Penzkofer D, Teske R, Dutzmann J, Koch A, Bielenberg W, Bonauer A, Boon RA, Fischer A, Bauersachs J, *et al*: Inhibition of miR-92a improves re-endothelialization and prevents neointima formation following vascular injury. Cardiovasc Res 103: 564-572, 2014.
18. Bellera N, Barba I, Rodriguez-Sinovas A, Ferret E, Asín MA, Gonzalez-Alujas MT, Pérez-Rodon J, Esteves M, Fonseca C, Toran N, *et al*: Single intracoronary injection of encapsulated antagomir-92a promotes angiogenesis and prevents adverse infarct remodeling. J Am Heart Assoc 3: e000946, 2014.
19. Liu Y, Li Q, Hosen MR, Zietzer A, Flender A, Levermann P, Schmitz T, Frühwald D, Goody P, Nickenig G, *et al*: Atherosclerotic conditions promote the packaging of functional MicroRNA-92a-3p into endothelial microvesicles. Circ Res 124: 575-587, 2019.
20. Bang C, Batkai S, Dangwal S, Gupta SK, Foinquinos A, Holzmann A, Just A, Remke J, Zimmer K, Zeug A, *et al*: Cardiac fibroblast-derived microRNA passenger strand-enriched exosomes mediate cardiomyocyte hypertrophy. J Clin Invest 124: 2136-2146, 2014.
21. Li S, Chen H, Ren J, Geng Q, Song J, Lee C, Cao C, Zhang J and Xu N: MicroRNA-223 inhibits tissue factor expression in vascular endothelial cells. Atherosclerosis 237: 514-520, 2014.
22. Livak KJ and Schmittgen TD: Analysis of relative gene expression data using real-time quantitative PCR and the 2(-Delta Delta C(T)) method. Methods 25: 402-408, 2001.
23. Li S, Geng Q, Chen H, Zhang J, Cao C, Zhang F, Song J, Liu C and Liang W: The potential inhibitory effects of miR-19b on vulnerable plaque formation via the suppression of STAT3 transcriptional activity. Int J Mol Med 41: 859-867, 2018.
24. Rabiolo A, Bignami F, Rama P and Ferrari G: VesselJ: A new tool for semiautomatic measurement of corneal neovascularization. Invest Ophthalmol Vis Sci 56: 8199-8206, 2015.
25. van Balkom BW, Eisele AS, Pegtel DM, Bervoets S and Verhaar MC: Quantitative and qualitative analysis of small RNAs in human endothelial cells and exosomes provides insights into localized RNA processing, degradation and sorting. J Extracell Vesicles 4: 26760, 2015.
26. Rehmsmeier M, Steffen P, Hochsmann M and Giegerich R: Fast and effective prediction of microRNA/target duplexes. RNA 10: 1507-1517, 2004.
27. Eisenreich A and Rauch U: Regulation and differential role of the tissue factor isoforms in cardiovascular biology. Trends Cardiovasc Med 20: 199-203, 2010.
28. Raposo G and Stahl PD: Extracellular vesicles: A new communication paradigm? Nat Rev Mol Cell Biol 20: 509-510, 2019.
29. Chen X, Yang F, Zhang T, Wang W, Xi W, Li Y, Zhang D, Huo Y, Zhang J, Yang A and Wang T: MiR-9 promotes tumorigenesis and angiogenesis and is activated by MYC and OCT4 in human glioma. J Exp Clin Cancer Res 38: 99, 2019.

30. Zhuang G, Wu X, Jiang Z, Kasman I, Yao J, Guan Y, Oeh J, Modrusan Z, Bais C, Sampath D and Ferrara N: Tumour-secreted miR-9 promotes endothelial cell migration and angiogenesis by activating the JAK-STAT pathway. EMBO J 31: 3513-3523, 2012.
31. Madelaine R, Sloan SA, Huber N, Notwell JH, Leung LC, Skariah G, Halluin C, Paşca SP, Bejerano G, Krasnow MA, *et al*: MicroRNA-9 couples brain neurogenesis and angiogenesis. Cell Rep 20: 1533-1542, 2017.
32. Zhang H, Qi M, Li S, Qi T, Mei H, Huang K, Zheng L and Tong Q: MicroRNA-9 targets matrix metalloproteinase 14 to inhibit invasion, metastasis, and angiogenesis of neuroblastoma cells. Mol Cancer Ther 11: 1454-1466, 2012.
33. Shyu KG, Wang BW, Pan CM, Fang WJ and Lin CM: Hyperbaric oxygen boosts long noncoding RNA MALAT1 exosome secretion to suppress microRNA-92a expression in therapeutic angiogenesis. Int J Cardiol 274: 271-278, 2019.
34. Eisenreich A, Bolbrinker J and Leppert U: Tissue factor: A conventional or alternative target in cancer therapy. Clin Chem 62: 563-570, 2016.
35. Versteeg HH, Schaffner F, Kerver M, Petersen HH, Ahamed J, Felding-Habermann B, Takada Y, Mueller BM and Ruf W: Inhibition of tissue factor signaling suppresses tumor growth. Blood 111: 190-199, 2008.
36. van den Berg YW, van den Hengel LG, Myers HR, Ayachi O, Jordanova E, Ruf W, Spek CA, Reitsma PH, Bogdanov VY and Versteeg HH: Alternatively spliced tissue factor induces angiogenesis through integrin ligation. Proc Natl Acad Sci USA 106: 19497-19502, 2009.